P7.11 DAYTIME CLOUD PROPERTY RETRIEVALS OVER THE ARCTIC FROM MULTISPECTRAL MODIS DATA

Douglas A. Spangenberg*
Analytical Services & Materials, Inc., Hampton, Virginia

Qing Trepte
Science Applications International Corporation, Hampton, VA

Patrick Minnis
NASA-Langley Research Center, Hampton, Virginia

Taneil Uttal
NOAA-ETL, Boulder, CO

1. INTRODUCTION

Improving climate model predictions over Earth's polar regions requires a complete understanding of polar clouds properties. Passive satellite remote sensing techniques can be used to retrieve macro and microphysical properties of polar cloud systems. However, over the Arctic, there is minimal contrast between clouds and the background snow surface observed in satellite data, especially for visible wavelengths. This makes it difficult to identify clouds and retrieve their properties from space. Variable snow and ice cover, temperature inversions, and the predominance of mixed-phase clouds further complicate cloud property identification. For this study, the operational Clouds and the Earth's Radiant Energy System (CERES) cloud mask (Trepte et al. 2002) is first used to discriminate clouds from the background surface in *Terra* Moderate Resolution Imaging Spectroradiometer (MODIS) data. A solar-infrared infrared near-infrared technique (SINT) first used by Platnick et al. (2001) is used here to retrieve cloud properties over snow and ice covered regions. Elsewhere, the visible-infrared solar-infrared split-window technique (VISST) developed by Minnis et al. (1995) is used to obtain the cloud properties. In the SINT algorithm, more accurate optical depths are achieved using the 1.6-μm near-infrared channel instead of the visible 0.65-μm channel because of the relatively dark snow and ice surface at 1.6 μm. Also, there is a much lower sensitivity of optical depth (OD) with changing 1.6-μm reflectance.

* *Corresponding author address:* Douglas A. Spangenberg, AS&M, Inc., Hampton, VA, 23666; e-mail: d.a.spangenberg@larc.nasa.gov

For those sunlit pixels tagged as being cloudy, either SINT or VISST is run to obtain both cloud macro and microphysical properties over the Atmospheric Radiation Measurement (ARM) Program North Slope of Alaska (NSA) Barrow site. These properties include OD, particle phase PP, effective ice crystal diameter D_e, ice water path IWP, effective liquid drop radius R_e, liquid water path LWP, and effective cloud height Z_{eff}. Minnis et al. (2004) give more information on the *Terra*-MODIS cloud property retrievals. The CERES-derived MODIS cloud amounts are validated using the cloud mask from the ARM-NSA micropulse lidar (MPL) based in Barrow. The cloud property retrievals from MODIS are evaluated by comparing them with retrievals obtained from the millimeter-wave cloud radar (MMCR) with additional data coming from the microwave radiometer (MWR) and Atmospheric Emitted Radiance Interferometer (AERI) for some of the radar retrieval techniques. All three instruments are based at the ARM-NSA Barrow site.

2. SATELLITE DATA AND METHODOLOGY

Terra MODIS 1-km near-infrared (1.6 μm), solar-infrared (3.7 μm), infrared (11 μm, T11), and split-window (12 μm) bands are used as input to the SINT algorithm to determine Arctic cloud properties over snow and ice scenes. Similarly, VISST, which replaces the near-infrared band replaced with the visible 0.65 μm reflectance, is run for those scenes without snow and ice. Only daytime retrievals are considered here. *Terra* overpasses centered at 1300 and 2000 local time (LT) passing over Barrow between March 2000 and June 2002. Snow and ice maps from the National Snow and Ice Data Center (NSIDC) or

from the National Oceanic and Atmospheric Administration (NOAA) Satellite Services Division (SSD) were used to determine whether to run SINT or VISST. The effective cloud height was determined from OD 11, and atmospheric temperature profiles from the Goddard Earth Observing System Version 4 (GEOS-4) global climate system model. Before comparing MODIS retrievals with those from the ground-based sensors, the satellite data were sub-sampled to 4-km then averaged over a 20-km radius circular region centered on Barrow. Figure 1 shows the geographic area surrounding Barrow used to obtain the spatial average of the MODIS retrievals. Note that much of this area lies over the Arctic Ocean. The 1-minute and 45-meter MMCR retrievals were averaged in terms of height, then over a 20-minute time window centered at the *Terra* overpass times.

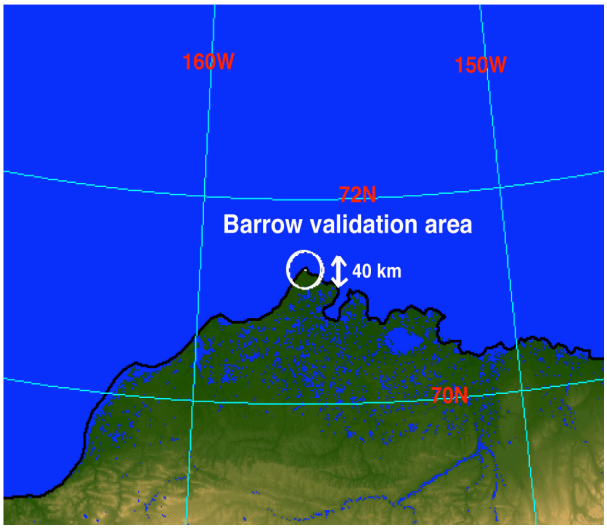

Figure 1. The geographic area surrounding Barrow used to validate the satellite retrievals. The circular region is 40-km in diameter.

3. RESULTS

Before obtaining the cloud macro and microphysical properties, the operational CERES cloud mask was used to discriminate clouds from the background snow and ice surface. Figure 2 shows the monthly-mean cloud amount (Ac) from CERES compared to the MPL cloud amount. The plot starts in March and ends in October since only sunlit scenes are considered where the solar zenith angle (SZA) is less than 82°. During this 2-year time frame from March 2000-April 2002, a total of 369 Terra overpasses were used. The lidar is more sensitive to all cloud types, and can be

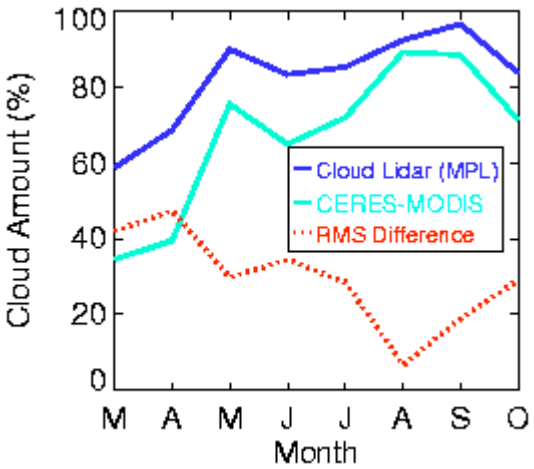

Figure 2. March 2000-April 2002 monthly-mean cloud amounts and RMS difference between Terra-MODIS and MPL over the ARM-NSA Barrow site.

expected to have somewhat higher values, as seen in the figure. Agreement is best during the late summer and autumn months, when the lidar cloud amounts are near 90%. The CERES-MODIS values underestimate the lidar *Ac* by no more than 10%. However, during the spring months, CERES values fall short of their MPL counterparts by 20-30%. This underestimate likely occurred because of the low sun conditions and frequent occurrence of hard-to-detect cirrus clouds over the cold snow and ice surface. The value of the 3.7-μm channel for cloud detection is diminished at large SZAs. The root-mean-squared (rms) difference between CERES and MPL is at a maximum of near 40 % in March and April and bottoms out to just under 10% in August.

The CERES-MODIS cloud properties were retrieved from SINT and VISST during the March 2000-June 2002 time frame. For cloudy pixels within 20 km of Barrow, the cloud properties were averaged and compared to a similar set of retrievals derived using a combination of the ground-based MMCR, MWR, and AERI measurements. Due to the requirement that both satellite and ground-based sensors must both report clouds, and because of the abundance of missing MMCR data, there was an average of 25 comparisons for any given month. Different radar techniques are used to retrieve cloud properties for ice (Matrosov, 1999; Matrosov et al. 2002) and liquid (Frisch et al. 1995) cloud phases. Since the radar-microwave radiometer-AERI (combined) retrievals are performed for less than 10% of the *Terra* overpasses, emphasis will be placed on the MMCR empirical, or regression, methods. Shupe et al. (2001) provide more information on the

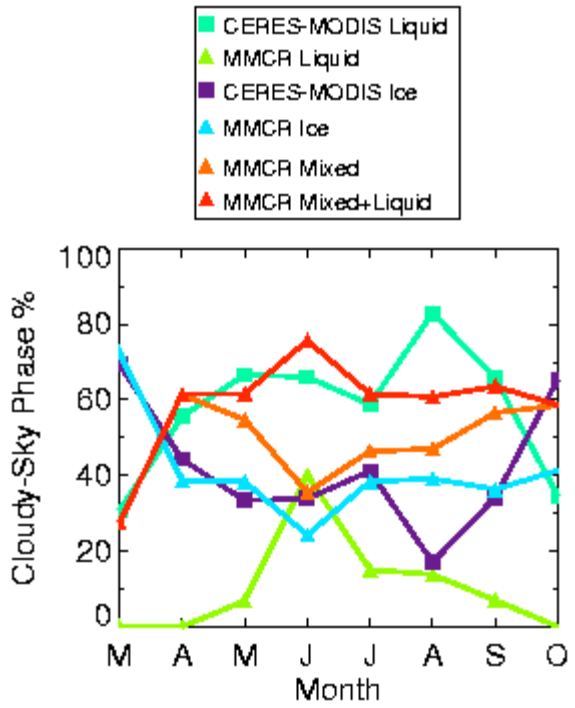

Figure 3. March 2000-June 2002 monthly-mean particle phase reported for Terra-MODIS and MMCR over the ARM-NSA Barrow site.

different radar techniques used to obtain the water contents and particle sizes.

The dominant MMCR cloud phase was found to be mixed and it occurred 40-60% of the time during the study period (Fig. 3). Only during March was the mixed-phase significantly less frequent than the ice phase. The dominant PP in the satellite retrievals was liquid in all months except March and October. Since the satellite cloud property retrieval techniques currently do not have the capability to identify mixed-phase clouds, the liquid phase would be expected instead; liquid drops tend to be found at the top of mixed-phase Arctic clouds (Rangno and Hobbs 2001). In order separate out mixed-phase clouds in the satellite data, the brightness temperature difference between 8.5 and 6.7 μm (T8.5-6.7) was compared to T11. Figure 4 shows the comparison for a selected set of 14 cases where a single phase was observed in MMCR, and the satellite had cloud returns generally over 75%. Notice how the mixed-phase MMCR cases lie between the all ice or all liquid phase. Given a much larger set of satellite images to derive robust statistics, it might be possible to classify those imager pixels falling between the ice and liquid data points as mixed phase.

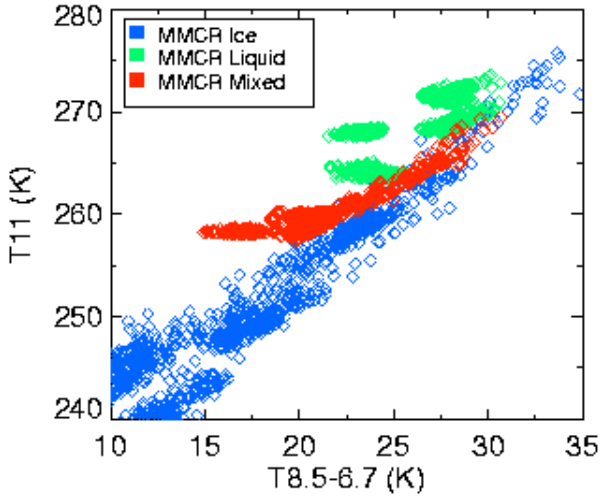

Fig. 4. MMCR phase and Terra-MODIS brightness temperature data for 14 selected cases where MMCR has a single phase in the time-height column.

Seasonal statistics of each cloud parameter were obtained over the Barrow validation area from March 2000 to June 2002. The results are presented in Table 1. Because of the higher number of valid data points and better agreement with the satellite retrievals, the MMCR regression (or empirical) methods were used in the statistical summary. Due to the lack of liquid-only clouds in the spring months, the OD-liquid, R_e, and LWP statistics are not reported in the table for that season. Examining *Ac*, values from the satellite and surface are highest in fall with values of 82 and 92%, respectively, with an rms difference of 23%. Spring and summer cloud amounts are 72 and 85% from the MPL, with the CERES cloud mask underestimating Ac by 23 % in spring and 14 % in summer. During all 3 seasons, comparing Z_{eff} to the radar middle cloud height yielded better agreement than for the radar tops, with the MODIS retrievals underestimating the surface-derived values by 1.2, 0.6, and 0.3 km in the spring, summer, and fall, respectively. The rms differences ranged from 1.8 in fall to 2.2 km in the spring. Optical depths, both liquid and ice, are consistently higher for the MODIS retrievals with the best agreement occurring in the summer for liquid and in spring for ice. The MODIS OD values are 8.7 and 1.7 for these two cases, respectively, with satellite biases of 3.1 for the liquid and 1.0 for the ice. If considering cases where ice was the only phase present in the time-height cross-section of the radar, CERES-MODIS over-estimates the MMCR values by 0.6 instead of 1.0.

Table 1. Seasonal MODIS and MMCR cloud property retrieval statistics for the time frame March 2000-June 2002. Sp=MAM, Su=JJA, and Fa=SO. The last column shows the particular radar method used to obtain the statistics.

Cloud Property	Satellite			Surface			Bias (Sat-Sfc)			RMS Diff			N			Surface Method
	Sp	Su	Fa	Sp	Su	Fa	Sp	Su	Fa	Sp	Su	Fa	Sp	Su	Fa	(M=MMCR)
Ac (%)	50	71	82	72	85	92	-23	-14	-10	40	30	23	171	140	78	MPL
Z_{eff}/Top (km)	1.5	2.5	2.2	4.8	5.6	4.6	-3.3	-3.1	-2.4	4.3	4.2	3.5	67	97	63	M-Top
Z_{eff}/Middle (km)	1.5	2.5	2.2	2.8	3.2	2.5	-1.2	-.6	- .3	2.2	1.9	1.8	67	97	63	M-Middle
OD-Liquid		8.7	12.3		5.6	8.4		3.1	3.9		9.9	11.2		35	10	M-VarN Regress
OD-Ice	1.7	3.3	4.7	0.7	1.1	0.9	1.0	2.2	3.8	4.9	6.5	9.4	34	38	37	M-Regress/1
D_e (μm)	63	49	63	93	106	93	-30	-57	-31	40	63	39	34	38	37	M-Regress
IWP (gm^{-2})	51	59	132	86	126	96	-35	-67	37	185	173	169	34	37	36	M-Regress
R_e (μm)		12.5	11.4		5.4	6.1		7.1	5.3		7.8	6.1		35	10	M-VarN Regress
LWP (gm^{-2})		84	93		51	67		33	26		72	71		35	10	M-VarN Regress

For the effective ice crystal diameter, the MMCR mean diameter (D_m) values were first converted into effective diameters using the equations

$$D_e = 27.5*(D_m)^{0.3};\ D_m >= 23.7\ \mu m, \qquad (1)$$

$$D_e = 3.0*D_m;\ D_m < 23.7\ \mu m. \qquad (2)$$

The effective ice diameters are consistently underestimated by MODIS compared to MMCR, with the best agreement occurring in spring and fall when the values are 63 μm for MODIS and 93 μm for MMCR. Again, differences in definitions, including those used in equations 1 and 2, must be reconciled before drawing any conclusions about the size differences. If only the pristine ice cases are considered when no other phase was observed in the radar, MODIS underestimates MMCR by only 19 and 12 μm in the spring and fall, respectively. For those 35 cases having liquid drops during summertime, MODIS retrieved a mean R_e of 12.5 μm whereas MMCR retrieved 5.4 μm, with an rms difference of 7.8 μm. While larger CERES-MODIS drops are not inconsistent with similar retrievals of R_e in Arctic clouds by Dong et al. (2001), in-cloud measurements are needed to determine which retrieval is more accurate. For IWP, the CERES-MODIS values are 51, 59, and 132 gm^{-2} in the spring, summer, and fall, respectively. These values are 35 gm^{-2} lower in the spring, 67 gm^{-2} lower in the summer, and 37 gm^{-2} higher in the fall compared to the MMCR retrievals. The rms differences are quite large, with values exceeding the means for each season. The MMCR retrieval methods produced some anomalously high IWP values as the data were not filtered below the 1000 gm^{-2} level, and this contributed to the large rms differences. If using only times with 100% ice in the MMCR column, the CERES-MODIS IWP values dropped by 25-30 gm^{-2} except in the summer, when they stayed nearly the same. Overall, however, the *IWP* statistics did not improve due to the unfiltered MMCR data and lack of cases where only the ice phase was present. Considering the LWP, satellite-retrieved values are 84 gm^{-2} in spring and 93 gm^{-2} in fall. These seasonal mean values exceed their MMCR counterparts by 33 and 26 gm^{-2}.

One of the improvements to the cloud property algorithm in polar regions will be the transitioning of NSIDC snow and ice maps to NOAA-SSD maps. Better snow and ice maps will allow for more accurate cloud detection and retrievals using MODIS data. The output product of NOAA-SSD has higher spatial resolution, includes reports of snow and ice cover not only from satellite data, but also from automated surface weather stations, and is manually adjusted, if necessary, on a daily basis (Ramsay 1998). Figure 5 shows an example of an ice map from May 31, 2004 from the NSIDC that CERES is currently using and one from the NOAA-SSD. The image is located over northern

Alaska and extends over the Arctic Ocean to the north of Russia. Note the higher spatial resolution of the NOAA product (Fig. 5d). The optical depth in Fig. 5f obtained using the NOAA-SSD map shows an improvement over the one obtained using the NSIDC map. Most improvements are to be expected at the coastline where the NSIDC has missing data, or where the maps have differing values of ice cover. Over inland Siberia, the NOAA-SSD snow map has much more coverage than the NSIDC map (not shown). This makes the resulting OD at the bottom-center of Fig. 5f much more continuous, with values between 4 and 16. Out over the open Arctic Ocean, where both ice maps have values above 75%, the difference in OD is more related to issues with the algorithm thresholds than with the maps themselves.

4. CONCLUSIONS AND FUTURE WORK

The CERES polar cloud-detection algorithm applied to *Terra*-MODIS data was able to capture most clouds seen in the MPL during the summer and fall seasons, with cloud amounts of 71 and 82 %, respectively. However, because of the presence of low sun and optically-thin cirrus clouds, the springtime cloud amount was 50%, a 23% underestimate. Using *Terra*-MODIS data, the SINT and VISST techniques were able to retrieve realistic cloud macro and microphysical properties over the ARM-NSA Barrow site for sunlit conditions. Ranges in the mean satellite cloud properties retrieved from March 2000-June 2002 for the ice phase include: D_e/53-85 μm, IWP/27-101 gm^{-2}, OD/1.1-3.5, and Z_{eff}/2.7-5.4 km. The corresponding values for liquid are: R_e/11.4-12.5 μm, LWP/84-93 gm^{-2}, OD/8.7-12.3, and Z_{eff}/0.6-0.9 km. The range of the cloud properties represents the differences attributed to the changing seasons. The satellite underestimate in cloud height of up to 0.3-1.2 km, if considering the geometric center of the cloud, was caused by an overestimated optical depth and lack of structure in the vertical temperature profiles.

With respect to PP, MMCR found that mixed-phase clouds are dominant at the NSA Barrow site except for March, when ice alone was the preferred phase. The VISST and SINT satellite retrieval techniques cannot presently discriminate the mixed phase from clouds containing either all ice or all liquid particles. Consequently, the satellite techniques predominantly retrieved liquid PP, which is expected because mixed-phase clouds typically have liquid droplets at their tops. Preliminary findings show that the MODIS 6.7, 8.5, and 11-μm brightness temperatures may be used to discriminate the mixed phase from all ice or all liquid scenes. The coastal location of Barrow, along with snow and ice contamination, made it difficult to accurately retrieve the cloud optical depth from space. Consequently, the *Terra*-MODIS optical depths represent overestimates of up to 2.5 for ice and 3.9 for liquid clouds. With respect to D_e, the satellite retrievals underestimate their radar-based counterparts by 12-46 μm. This likely occurred because of differences in size definitions and because some of the clouds examined had much larger crystals near cloud base. Finally, R_e values retrieved from the MMCR appear to be small compared the MODIS-retrieved values. To confirm this, in situ aircraft sampling of cloud drop sizes is needed. It should be pointed out here that there are inherent errors in the ground-based MMCR retrievals of 40% for D_e, 75% for IWP, 30% for R_e, and 40% for LWP. These errors likely contribute to some of the discrepancies between MODIS and MMCR cloud property retrievals observed here.

For future work, adjustments will be made to the CERES cloud mask algorithm to capture more clouds during the cold season. Improved snow and ice maps from NOAA-SSD will be used to improve the cloud mask and for determining whether to run SINT over snow and ice scenes or VISST for open land or ocean. Also, the discrepancies between the satellite and surface retrieved particle sizes needs to be resolved. Aircraft particle size measurements from the planned Mixed-Phase Arctic Cloud Experiment will be a valuable source of data to continue this study. To view cloud properties at ARM-NSA and other ARM sites, please see the web page, http://www-pm.larc.nasa.gov.

5. REFERENCES

Dong, X., G.G. Mace, P. Minnis, and D.F. Young, 2001: Arctic stratus cloud properties and their effect on the surface radiation budget: Selected cases from FIRE ACE. *J. Geophys. Res.*, **106**, #D14, 15,297-15,312.

Frisch, A.S., C.W. Fairall, and J.B. Snider, 1995:Measurements of stratus cloud and drizzle parameters in ASTEX with a Ka-band Doppler radar and microwave radiometer. *J. Atmos. Sci*, **52**, 2,788-2,799.

Matrosov, S.Y., 1999: Retrievals of vertical profiles of ice cloud microphysics from radar and IR measurements using tuned regressions between reflectivity and cloud parameters. *J. Geophys. Res.*, **104**, 16,741- 16,753.

Matrosov, S.Y., A.V. Korolev, and A.J. Heymsfield, 2002: Profiling cloud ice mass and particle characteristic size from doppler radar measurements. *J. Atmos. Ocean. Technol.*, **19**, 1,003-1,018.

Minnis, P., et al., 1995: Cloud Optical Property Retrieval (Subsystem 4.3). In *Clouds and the Earth's Radiant Energy System (CERES) Algorithm Theoretical Basis Document, Vol. III: Cloud Analyses and Radiance Inversions (Subsystem 4), NASA RP 1376 Vol. 3*, edited by CERES Science Team, pp. 135-176.

Minnis, P., D. F. Young, S. Sun-Mack, P. W. Heck, D. R. Doelling, and Q. Z. Trepte, 2003: CERES cloud property retrievals from imagers on TRMM, Terra, and Aqua. *SPIE 10th Intl. Symp. Remote Sens., Conf. on Remote Sens. Clouds and Atmos.*, Barcelona, Spain, September 8-12, 37-48.

Platnick, S.J., Y. Li, M.D. King, H. Gerber, and P.V. Hobbs, 2001: A solar reflectance method for retrieving cloud optical thickness and droplet size over snow and ice surfaces. *J. Geophys. Res.*, **106**, #D14, 15,185-15,199.

Ramsay, B. H., 1998: The interactive multisensor snow and ice mapping system. *Hydrol. Process.*, **12**, 1,537-1,546.

Rangno, A.L. and P.V. Hobbs, 2001: Ice particles in stratiform clouds in the Arctic and possible mechanisms for the production of high ice concentrations. *J. Geophys. Res.*, **106**, #D14, 15,065-15,075

Shupe, M.D., T. Uttal, S.Y. Matrosov, and A.S. Frisch, 2001: Cloud water contents and hydrometeor sizes during the FIRE Arctic Clouds Experiment. *J. Geophys. Res.*, **106**, #D14, 15,015-15,028.

Trepte, Q.Z., P. Minnis, and R.F. Arduini, 2002: Daytime and nighttime polar cloud and snow identification using MODIS data. *Proc. SPIE Conf. on Optical Remote Sens. of the Atmosphere and Clouds III*, Hangzhou, China, Oct. 23-27.

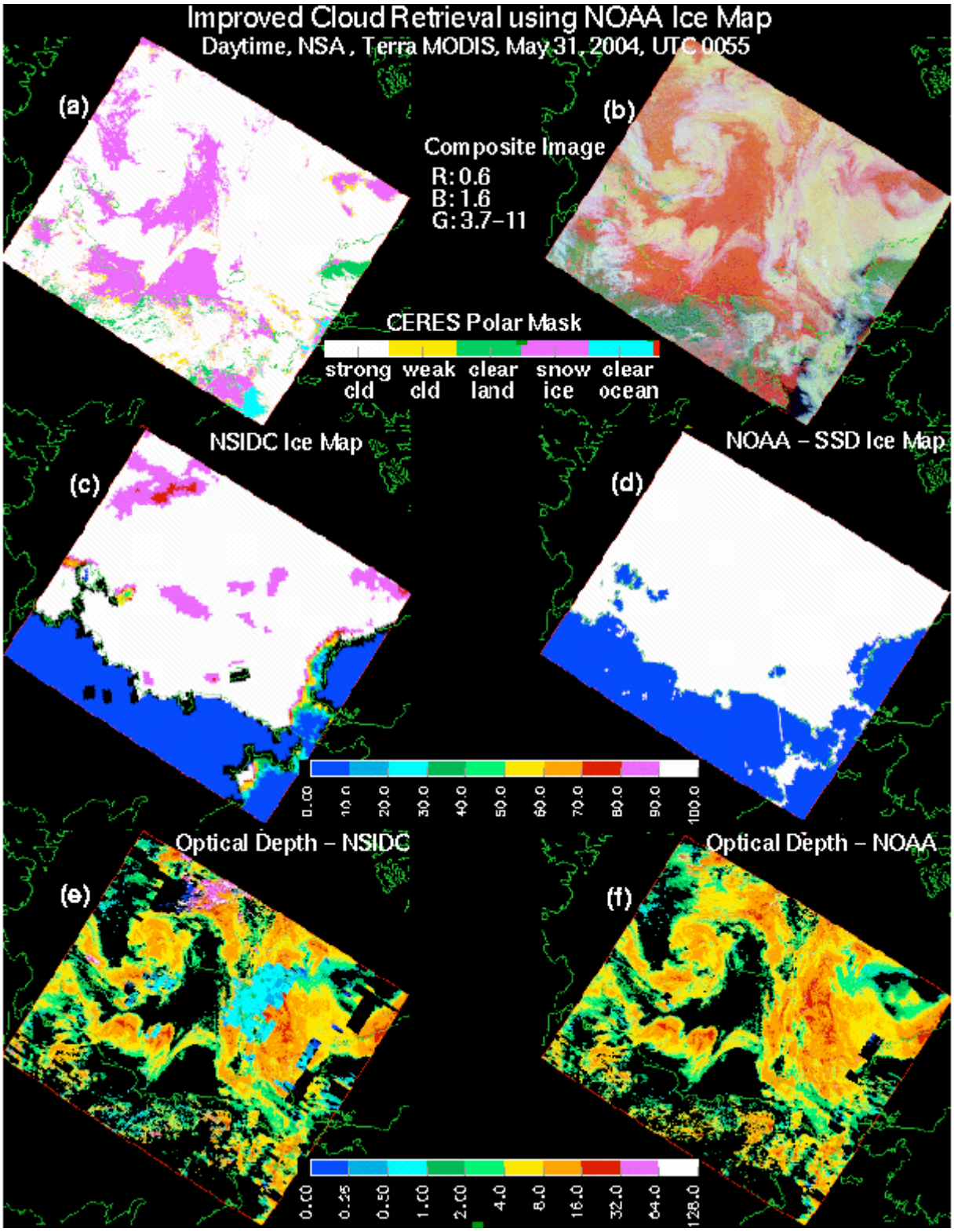

Figure 5. Cloud OD retrievals on May 31, 2004, 00:55 UTC using the NSIDC ice map and NOAA-SSD ice map. The region extends from northern Alaska on the bottom-right to the Arctic Ocean north of Russia on the upper-left.